

Virtual Engineering Centre – Examples of Virtual Prototyping and Multidisciplinary Design Optimization

J.E. Cooper, G. Abdelal, N. Cameron, M. Fisher, J. Forrest, G. Georgiou, K.K.B. Hon, M. Jump, G.D. Padfield, A.J. Robotham, F. Shao, M. Webster, M.D. White.

Virtual Engineering Centre, University of Liverpool, STFC – Daresbury Laboratory
Daresbury Science & Innovation Campus
Warrington, WA4 4AD, UK

j.e.cooper@liverpool.ac.uk

ABSTRACT

The requirement for the use of Virtual Engineering, encompassing the construction of Virtual Prototypes using Multidisciplinary Design Optimisation, for the development of future aerospace platforms and systems is discussed. Some of the activities at the Virtual Engineering Centre, a University of Liverpool initiative, are described and a number of case studies involving a range of applications of Virtual Engineering illustrated.

1.0 INTRODUCTION

The North West region of England has a high concentration of aerospace businesses serving both civil and military customers across the world and, despite the recent economic downturn, the long-term business prospects for the aerospace sector are very encouraging and offer these businesses excellent opportunities for growth [1]. However, aerospace product development is an increasingly more complex and globalised activity involving a world-wide supply chain. If the challenging performance goals for all new aircraft platforms and the engineering systems on which they are built are to be met then it is imperative that developers adopt effective system engineering processes to create the innovative solutions expected.

INCOSE [2] consider Systems Engineering to be “*an interdisciplinary process to ensure that the customer and stakeholder's needs are satisfied in a high quality, trustworthy, cost efficient and schedule compliant manner throughout a system's entire life cycle*” and their systems engineering process SIMILAR involves seven tasks: State the problem, Investigate alternatives, Model the system, Integrate, Launch the system, Assess performance, and Re-evaluate.

Modelling is a fundamental aspect of systems engineering. Models are required for both the product and the process because systems engineering is responsible for both the product and the process that produces it. Virtual Engineering (VE) is concerned with integrated product and process modelling, where product models embody the design data, developed through process models. The product models being used by developers are increasingly more complex and demand the integration of mechanical, electrical and software systems into a single, holistic product modelling system linked to requirements and performance data. A product model embedded within a synthetic environment of the relevant life cycle phase is described as a Virtual Prototype (VP), as shown in Figure 1.

The elements of the VP are derived from Hubka's Theory of Technical Systems [3] and include the engineering system (TS), the active environment (En) and the human operator (Hu). All three elements interact with each other and influence the effectiveness of the transformational process that is being represented. As a consequence, VPs can be used to evaluate the functionality and behaviour of an engineering system in its context of use and determine how the requirements are being satisfied.

VIRTUAL ENGINEERING CENTRE

The real advantage is that the VP can serve as the basis for, not only demonstrating compliance with requirements, but also optimising the design and developing and validating the requirements themselves. Research cited by INCOSE indicates that effective use of virtual/systems engineering can save 10-20% of project budgets[4].

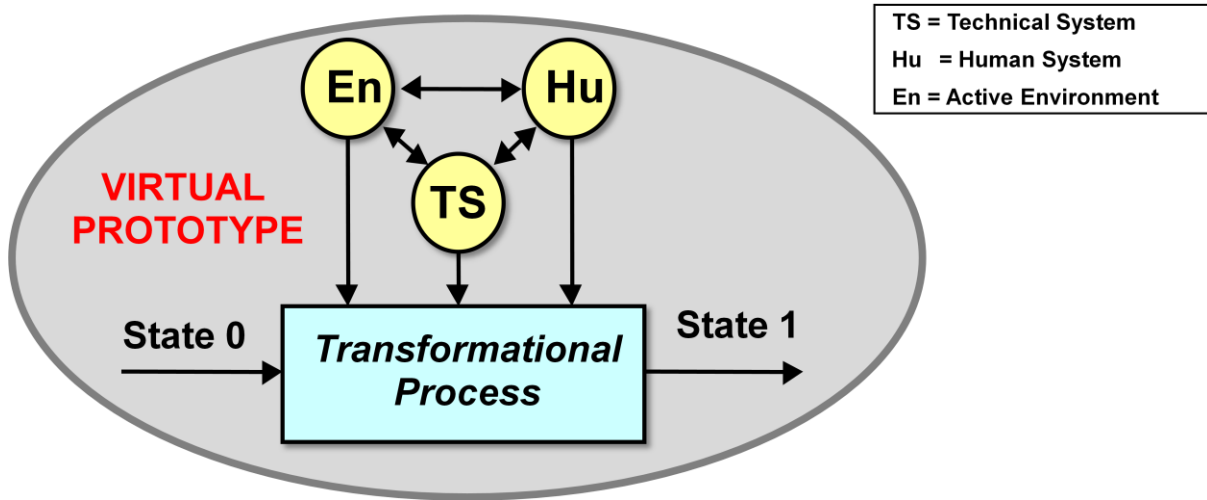


Figure1: Principal elements of a Virtual Prototype

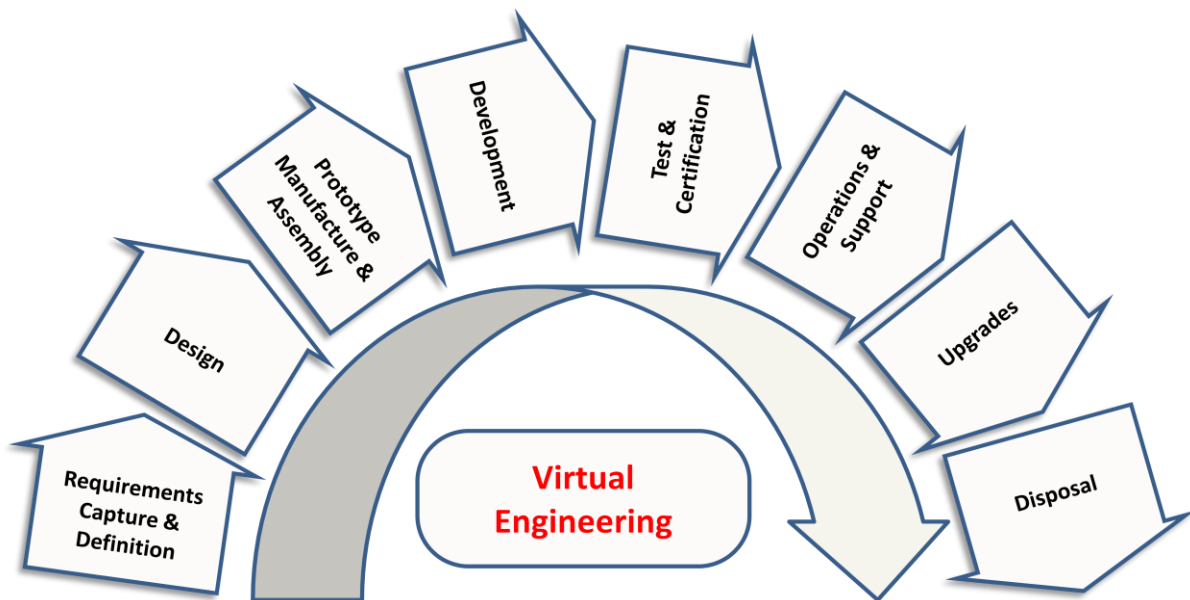


Figure 2. Virtual Engineering - Integrating Requirement Capture with Design and Virtual Prototyping through all Elements of the Product Life Cycle

VPs can be regarded as powerful development tools. However, to ensure that customers and stakeholder needs are satisfied throughout the product’s life cycle requires, many such VPs need to be developed in order to meet the multitude of requirements that define the functionality and operational capability of the engineering system across the product life cycle. Virtual Engineering (VE) is the creation and exercise of VPs at the front-end of the life cycle, shown in Figure 2, which will continue to serve purpose and support decision making throughout the life cycle.

This paper describes the Virtual Engineering Centre at the University of Liverpool which has been set up as a centre of excellence in Virtual Engineering. A number of case studies demonstrating the application of Virtual Engineering, in no particular order, are described.

2.0 VIRTUAL ENGINEERING CENTRE

The Virtual Engineering Centre (VEC) is a University of Liverpool initiative in partnership with the Science and Technology Facilities Council Daresbury Laboratory, Northwest Aerospace Alliance, BAE Systems, Morson Projects and Airbus UK. The main objective of the VEC is to create a centre of excellence in Virtual Engineering that will significantly improve the overall business performance of the aerospace sector in the North West region of England and so is partially funded by the Northwest Regional Development Agency and the European Regional Development Fund.

The VEC will provide integrated product/process model and virtual prototyping capabilities and facilities for the benefit of industrial organisations of *all* sizes throughout the supply chain to design and evaluate rapidly new products, production facilities or services in virtual form. The VEC will provide a VE research focus through the creation of multidisciplinary teams working collaboratively and concurrently across industry and academia. This multidisciplinary approach will push the boundaries of existing capabilities resulting in high fidelity simulation for scenarios not currently possible. The VEC will help fill the shortfall in graduate engineers with a working knowledge and capability in VE and use real-world product and process model data to create demonstrations and case studies that demonstrate the business benefits of VE to the aerospace supply chain. To help achieve these aims, the VEC has access to a high concentration of aerospace businesses, some of UK's most capable research teams in academia and, through the STFC Daresbury Laboratory, computational power at a level able to tackle the massive complexities of VE required for new aerospace systems.

The activities within the VEC are structured in a framework of five technical work packages (WP), a skills development work package (WP6), and a business development/knowledge exchange work package (WP7) as shown in Figure 3:

- a) WP 1 – Lifecycle VE integration.
- b) WP 2 – VE for manufacturing and assembly.
- c) WP 3 – VE for development and certification.
- d) WP 4 – VE for operations and support.
- e) WP 5 – Verification and validation of VE processes and practises.
- f) WP 6 – VE for Life.
- g) WP 7 – VE for Business.

The technical work packages (WP2, WP3 and WP4) will develop state of art VE practice for use in the relevant phases of the product life cycle (Figure 2), whilst WP1 will establish an integrated product and process modelling framework to support VE practice at all levels of skills and competencies throughout the product life cycle. WP5 will develop a framework for verification and validation (V&V) of VE and VPs, drawing from Research Council funded activities at the University of Liverpool. Technical Work Packages WP2, WP3, and WP4 will develop VPs to demonstrate product and process modelling capabilities. They will each have the following VE objectives relating to their distinct phase of the product life cycle:

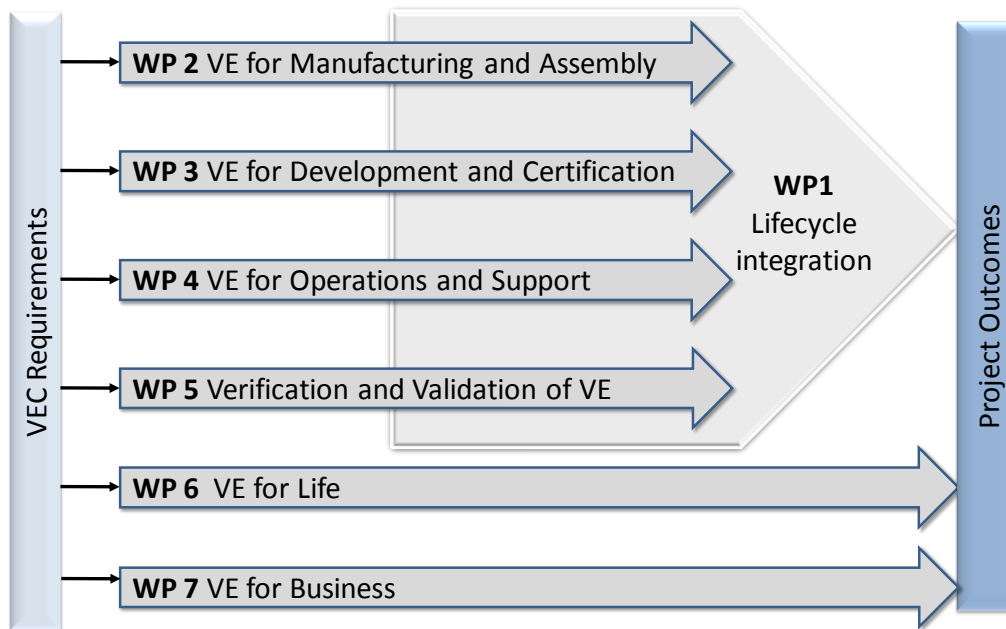


Figure 3. Work Package Delivery Structure Schematic

1. Create a database for an existing baseline design case, including legacy requirements set.
2. Create a baseline product model.
3. Develop a process model for populating the product model.
4. Develop requirements for a 'new' design providing an upgraded capability beyond the baseline.
5. Use the process model to populate product models with new data to examine candidate solutions to meet new requirements and iterate to explore trade-offs in requirements matching.
6. Create a virtual prototype using the product model and associated synthetic environments
7. Conduct demonstrations to a 'virtual' customer.
8. Set up VE exercises that serve as client demonstrations and educational tools.

3.0 COMPOSITES CURING MODELLING

Autoclave processing is one of the oldest composites processing technologies. In this process, plies or prepregs or tapes (fibres that are pre-impregnated with the resin) are stacked on the surface of the tool. They are then subjected to high pressure and temperature to allow the stacks to become a single coherent structure by forcing out air pockets and excess resin. The process is carried out in an autoclave, which is a large pressure vessel with an integral heating element. One can think of an autoclave as an oven that can be pressurized. Not unlike a pressure vessel, it is usually constructed as a cylindrical tube with a door at one end. Its main function is to provide the heat and pressure necessary to consolidate and cure composite structures.

The main objective of this project is the early prediction of composite part deformations during autoclave manufacturing. These deformations will help us to modify autoclave-tool design to minimize it within specified tolerances (customer requirements). Numerical autoclave simulation will reduce the cost of the iterative manufacturing process to find the optimized autoclave-tool design. Three software packages will be used during this project: CATIA is used to model the part and tool designs, ABAQUS is used to perform the Autoclave simulation applying finite element technique, and Fortran 11 is used for programming user-subroutines that model special material properties.

Autoclave simulation consists from three components. The first component is the Thermo-Chemical model to simulate the curing cycle and determine the temperature and degree of cure distributions as a function of the cure cycle time. Second component is a Resin Flow Analysis to determine the final fiber volume fraction after removal of excess resin under autoclave pressure. Third component is the stress-thermal model to calculate residual stresses (that can affect part fatigue life) and deformation (that can affect assembly process).

3.1 Thermo-Chemical model

Equation (1) is modelled applying the finite element technique (ABAQUS). A transient thermal analysis is performed that includes element conductivity, internal heat generated by epoxy during cure, and convection to the air in the Autoclave (convection term is not shown in the equation)

$$\rho c_p \frac{\partial T}{\partial t} = \frac{\partial}{\partial x_i} \left(k_{ij} \frac{\partial T}{\partial x_j} \right) + \rho H_R \frac{\partial c}{\partial t} + Q_v \quad (i, j = 1, 2, 3) \quad (1)$$

where ρ denotes the composite density, c_p the specific heat, T the temperature, t the time, x_i the coordinates, k_{ij} the components of the thermal conductivity tensor, and c the degree of cure, which is defined as the ratio of the heat released by the reaction to the ultimate heat of reaction H_R . The fabric thermal conductivity tensor and the cure kinetic model need to be supplied for this model.

3.1.1 Fabric thermal conductivity tensor

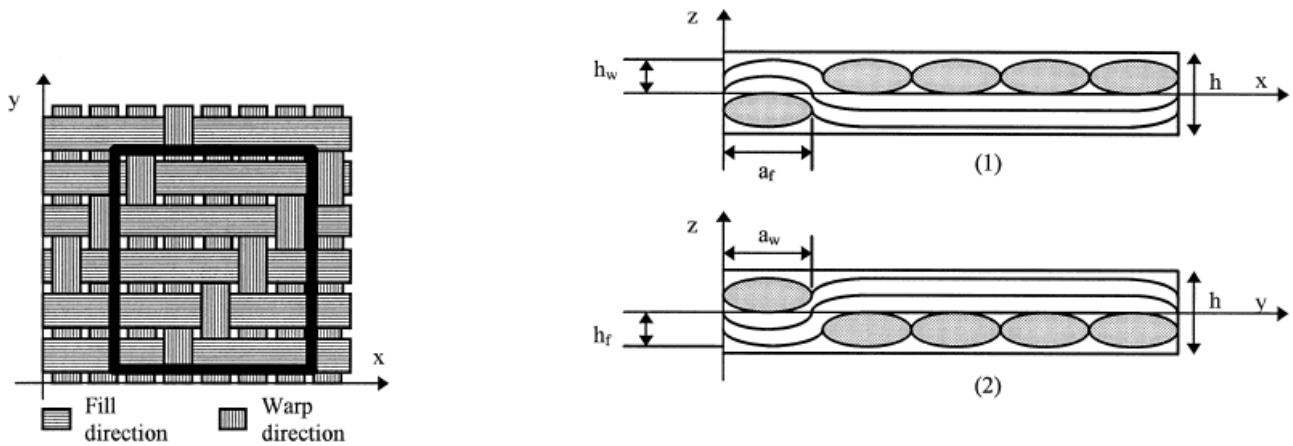


Figure 4. Five-harness satin weave. (a) Unit cell; (b) fiber undulation in fill and warp direction.

For in-plane thermal conductivity, closed analytical models are available but only for plain-weave, which is based on a micromechanics model that is based on the thermal-electrical analogy and it will take some time to extend it to 5-harness satin weave shown in Figure 4. There is an analytical model for the satin weave to model the transverse thermal conductivity. The other method applied in this area, is a finite element model of the unit-cell of the 5-harness satin wave and run steady-state heat transfer analysis to predict the thermal conductivity tensor.

We have two options to predict the thermal conductivity tensor: the first option is to use the experimental data sheet from the fabric supplier. The second option is to predict the thermal conductivities of 5-harness satin weave composite, by modeling a unit cell using 3-dimensional finite elements, considering the interlaced fiber tow architecture microscopically. At the unit cell boundary, the corresponding periodic boundary conditions are applied. The model can be verified by the use of the available analytical model prediction of the transverse thermal conductivity.

If the finite element approach is used then the following input parameters are required:

- Thermal conductivity of the resin and fibres.
- Width of the fill and warp strands (mm).
- Maximum thickness of the fill and warp strands (mm).
- Thickness of the unit cell (mm), which equals the lamina thickness.
- Strand volume fraction in the composite.
- Fiber volume fraction in the strand.
- Fiber volume fraction in the composite.

3.1.2 Cure Kinetic Model

The last term in transient-thermal Equation (1) corresponds to the internal heat generation associated with the exothermic cure reaction, and is described by a cure kinetics model

$$\frac{d\alpha}{dt} = K\alpha^m(1-\alpha)^n \quad K = Ae^{-\Delta E/RT} \quad (2)$$

where Equation (2) represents some function of T and α , and takes on specific forms depending on the material system under consideration. This form requires the definitions of 6-constants, which can be available in literature or provided by the fabric supplier. These constants are most often determined using isothermal and/or dynamic DSC measurements and various curve-fitting techniques.

The required experimental work, a total of eight additional DSC (differential scanning calorimetry) ‘scans’ were performed. Of these, 6 were isothermal tests, two at each of 130 °C, 150 °C, and 170 °C. In these tests, the specimens were heated rapidly to the desired temperature where they were maintained for a total of 2 hours, then rapidly cooled. Two dynamic DSC scans were also performed in which specimens were heated at rate of 10 °C/minute from room temperature to about 290 °C at which point the cure was essentially complete.

3.2 Resin Flow Analysis

Hubert [5] showed that in the autoclave process, flow of the matrix resin is induced to remove excess resin from the laminate, promote bonding between plies, and collapse any voids within the laminate. This flow process may also play an important role in the development of residual stress and deformation. Even in flat laminates, non-uniform resin distribution through the part thickness may develop due to an imperfect compaction process.

V.A.F. Costa developed a three-dimensional numerical model to simulate and analyze the mechanisms dealing with resin flow, heat transfer and the cure of thick composite laminates during autoclave processing. The model, which incorporates some of the best features of models already reported in the literature, is based on the Darcy law, the convection-diffusion heat equation, and appropriate constitutive relations.

The same approach will be applied in our simulation, but instead of simulating the equations using finite-volume approach, the flow module in ABAQUS will be used.

Input parameters required for this process are:

- Fiber volume fraction in composite.
- Resin viscosity model as a function of temperature and degree of cure.
- Resin degree of cure at gelation.

3.3 Stress-Thermal Model

During autoclave processing, a number of different processes lead ultimately to the development of residual stress and deformation. The mechanism for stress development in this case is the combination of these thermal strains with changing resin modulus. Unless both are present, no residual stress and deformation will be generated.

From the mechanisms for the development of process-induced stress and deformation described in the literature, five main sources have been identified:

- Thermal strains (major).
- Resin cure shrinkage strains (minor).
- Gradients in component temperature and resin degree of cure (major).
- Resin pressure gradients (resulting in resin flow) (minor).
- Tooling mechanical constraints (major).

Residual stress and deformations calculations applying sequential transient stress-thermal analysis in ABAQUS, involve two main issues;

- Viscoelastic material model to simulate the resin behavior with temperature and degree of cure.
- Micromechanical model to predict the Elasticity tensor of the composite part with time as a function of the fiber and resin material properties.

3.3.1 Viscoelastic Material Model

Characterization of the Viscoelastic response of a composite material is a complex problem, and is doubly difficult for a curing composite. The most serious difficulties arise from the need to measure material behavior over a wide range of temperatures and degrees of cure and the fact that curing of the resin changes its material response even as it is being tested. The amount and type of data collected, and the characterization method used depends on the Viscoelastic model chosen.

The isotropic matrix resin in composite materials is modeled as a so-called ‘cure-hardening/instantaneously linear elastic’ (CHILE) material. This designation indicates that the modulus of the instantaneously linear elastic resin increases monotonically with the progression of cure. Two models for prediction of resin modulus development are employed here, one from Bogetti and Gillespie [6] and another developed by Johnston [7].

The estimation of the CHILE model parameters, requires searching literature for stress-relaxation test data of the specified epoxy (Hexcel material 914), or performing a set of tests defined by Johnston [7]. The test in this case was performed using a Rheometrics RMS-800 rheometer on an 8-ply unidirectional specimen (fibers aligned with the twist axis) with approximate dimensions of 45 mm x 12.5 mm. The applied strain was varied from 1% to 10% with a frequency of 10 rad/s.

Input parameters are:

- Fibers mechanical properties (Transverse Isotropic) [E11 - E22 - G13 - G23 - ν].
- Resin mechanical properties (isotropic) [E - ν], for fully cured and at room temperature.
- Any material data at higher temperature or different degree of cure is welcome.

3.3.2 Micromechanical Model

A micromechanical model called MESOTEX [8], which was developed by Université de Technologie de Compiègne and Atelier Industriel de l’Aéronautique de Cuers Pierrefeu in FRANCE, will be used for prediction of the instantaneous elastic behavior of composites reinforced with satin weave fabrics. By using

the classical thin laminate theory applied to each woven structure, this analytical model takes into account the strand undulations in the two directions and also integrates the geometrical and mechanical parameters of each constituent (resin, fill and warp strands). A representative volume is chosen for the woven composite and the fiber architecture is described by several functions.

Input parameters required are:

- Fibers mechanical properties (Transverse Isotropic) [E11 - E22 - G12 - G23 - ν].
- Lamina parameters that already defined for the Thermal-Chemical model.

Simulation results of autoclave curing of composite part are shown in Figures 5 and 6.

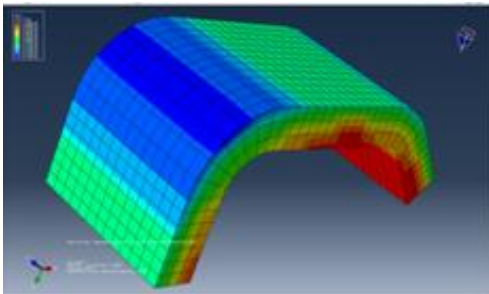


Figure 5. Degree of Cure Distribution.

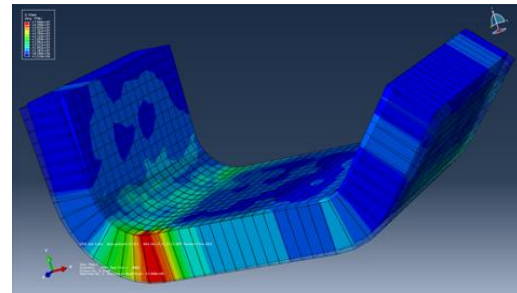


Figure 6. Spring-back of Composite Part due to Residual Stresses.

4.0 AEROELASTICITY / CFD

4.1 Aeroelastic Analysis

The conceptual design of aircraft prototypes provides the ability to perform collaborative and multidisciplinary analyses in an effort to explore the worthiness of potential designs. In this direction, the initial shaping of the Very Large Transport Aircraft prototype (VeLTA) was carried out through using an aero-structural sizing tool called NeoCASS [9], facilitating the creation of structural and aerodynamic models (Figure 7) and easing the submission of relevant analyses.

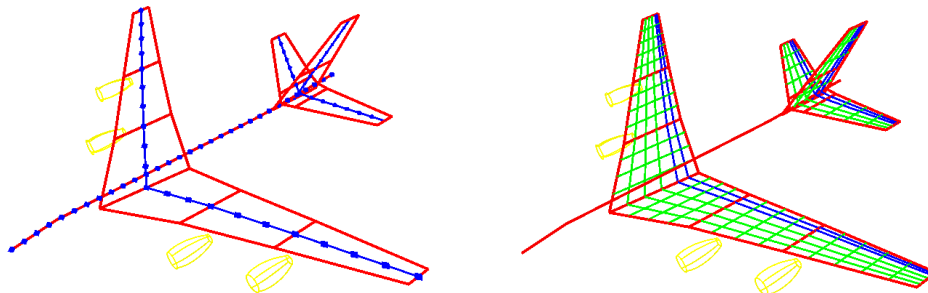


Figure 7. Structural and aerodynamic elements in the VeLTA model.

More specifically, the combined structural and aerodynamic model of VeLTA was investigated for flutter instabilities at a flight condition where the Mach number was selected to be $M_\infty=0.5$ and the air density $\rho=1.225\text{kg/m}^3$, while the aerodynamic forces were calculated using the following reduced frequencies $k=0.0001, 0.01, 0.05, 0.1, 0.2, 0.4, 0.6, 0.8$. The obtained frequency and damping ratio trends of the first five flexible modes for the VeLTA model are depicted at Figure 8. A typical flutter mechanism occurs when the damping ratio curve crosses the horizontal axis and this dynamic instability was observed from the coupling of the third and fourth mode, resulting to a flutter speed of 281.52m/s.

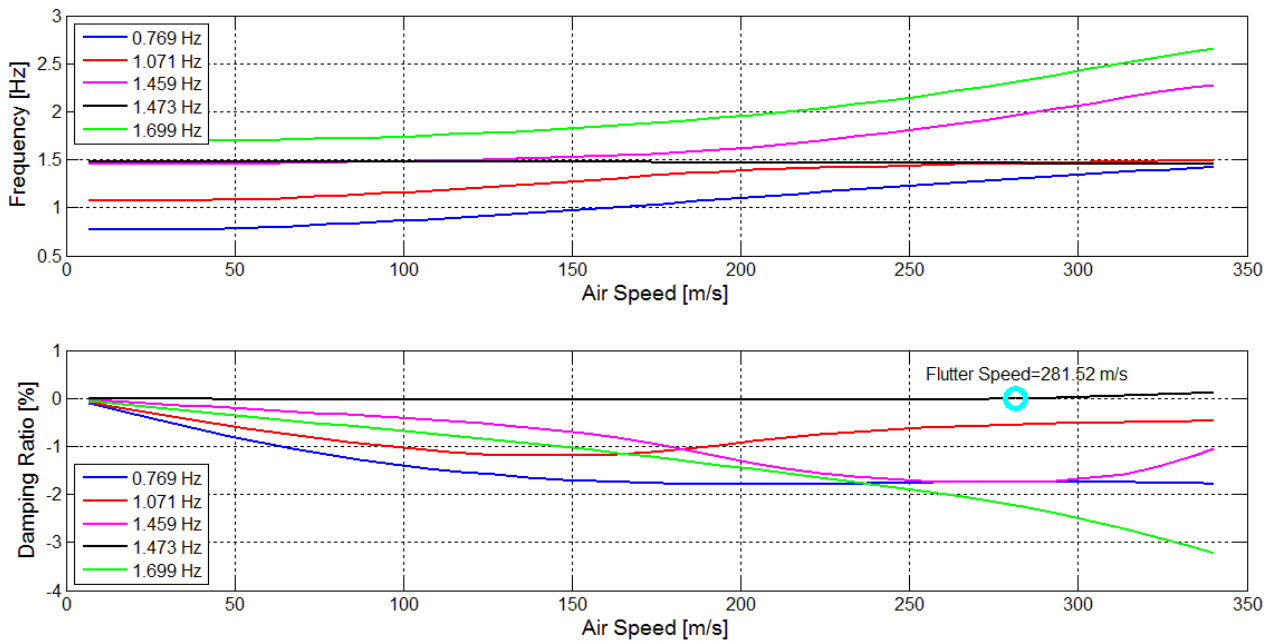


Figure 8. Frequency and damping ratio trends versus air speed for VeLTA model.

4.2 CFD Modelling

One of the main goals of the VeLTA prototype study is to develop a high-fidelity flight model of the aircraft, for use in a real-time simulation environment. A key component of the flight model is the aerodynamic database which has a major influence on both the static and dynamic behaviour of the aircraft. CFD has been used to derive the main wing aerodynamic properties, through analysis of two-dimensional aerofoil sections using the ANSYS Fluent solver. Lift, drag and moment coefficients have been obtained at two degree angle-of-attack intervals, through the use of automated scripting routines. This has enabled the aerodynamic database to be built in an efficient manner.

A further goal of this study is to use the VeLTA geometry as a test-bed, on which multiple aerodynamic optimisation studies can be performed using CFD. A first step in this process is the validation of the tools and methodologies used during the CFD simulations. Gridgen's 'Pointwise' meshing tool and the ANSYS Fluent solver have been adopted as the tools of choice at the VEC, therefore a validation exercise has been performed to ensure that this combination produces reliable results. The NASA 'High-Lift Prediction Workshop' test-case [10] was chosen as it involves a trapezoidal wing with fully deployed slats and flaps. Not only was this a challenging test-case, but it represented a similar flow regime to the high-lift landing configuration that is core to the development of the VeLTA prototype.

Figure 9 shows lift and drag as a function of angle-of-attack for the trapezoidal wing, with a comparison between the NASA wind tunnel results and those obtained using ANSYS Fluent. It can be seen that the CFD data follows the lift curve slope well, despite a slight under-prediction of lift. The onset of stall is captured very well, with the post-stall region also showing excellent agreement. Similarly, the drag curve shows excellent agreement at all angles-of-attack.

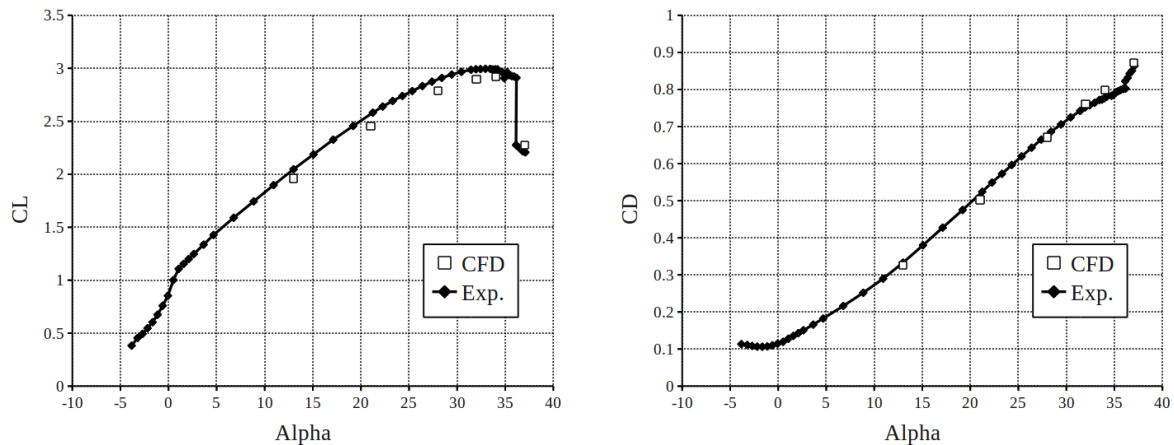


Figure 9: Comparison of $C_L-\alpha$ (left) and $C_D-\alpha$ (right) between wind tunnel and CFD results for the NASA High-Lift Prediction Workshop three-element trapezoidal wing.

Following successful validation of the CFD tools, a high-lift version of the VeLTA model has been developed, with a leading edge droop-nose device, two leading edge slats and a trailing edge Fowler flap on each wing. The surface mesh is shown on the left side of Figure 10. CFD simulations on this model are ongoing, with preliminary flow visualisation results shown on the right side of Figure 10. It is anticipated that the CFD model of VeLTA will be used to verify results from the flight dynamics model and investigate certain non-linear aerodynamic phenomena.

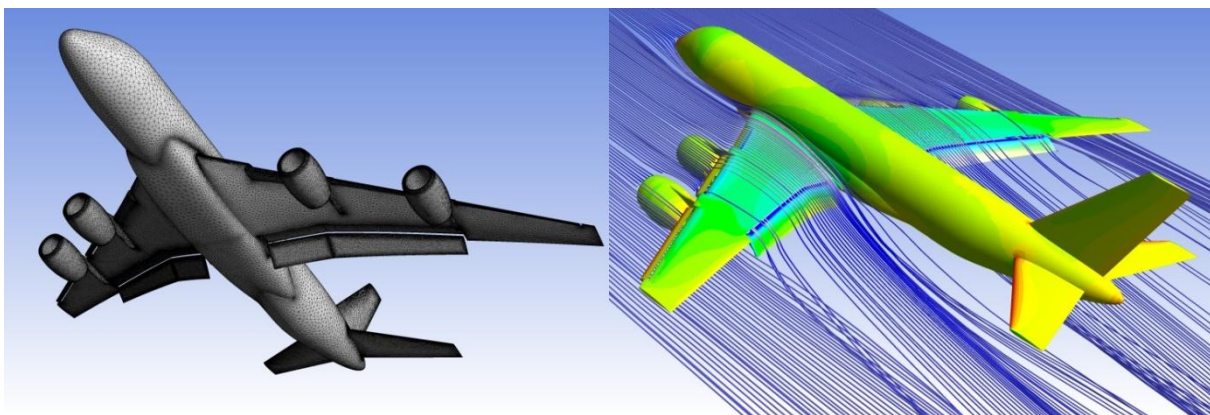


Figure 10: Images derived from CFD modelling of the VeLTA prototype. Surface mesh (left); pressure contours and flow streamlines (right).

5.0 UNCERTAINTY IN THE RIVETING PROCESS

5.1 Finite Element Modelling

Fox and Withers [11] performed experimental work to measure strains on a one-rivet sample using Synchrotron X-ray and neutron diffraction. Based on his work, we developed two schemes to simulate residual stresses due to one rivet, which will be the base of our modeling for a test case with multiple rivets. The scheme applied here is based on work done by Jachimowicz [12], where he assumes orthotropic thermal expansion of the rivet (axial-radial-tangential), then applies the temperature boundary condition on the rivet to simulate the expansion and contraction of the rivet. Temperature boundary conditions were selected based on the work done by Repetto (270 C). In scheme No.1 we neglected any

heat transfer between rivet and panel and performed static analysis applying boundary conditions that are shown in Figure 11. In scheme No.2 we included the effect of heat generated due to fast rivet deformation.

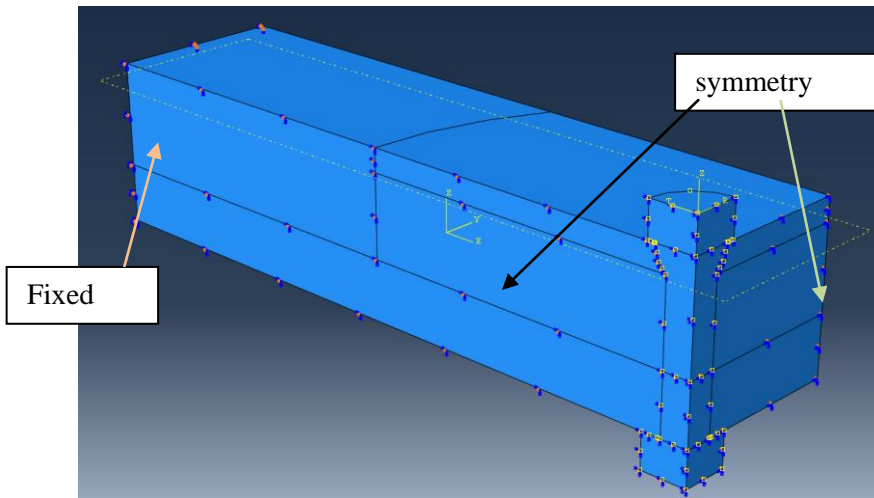


Figure 11. Boundary Condition Scheme used for the One-Rivet Sample.

The boundary conditions are applied at faces and the temperature is applied as a boundary condition on the rivet. Tangential and radial stresses along distance from rivet centre at depth of the countersink for the Schemes No. 1, No. 2 and experimental results are shown in Figure 12. The objective of this step is to verify that the average stresses are equal. Modelling the exact residual stresses due to riveting process requires the use of Explicit analysis which requires very long running time. Improving numerical results requires the application of an optimization routine and substructure Technique. Results can be further improved by including contact analysis which includes thermal contact conductance definition that can be defined using the Yovanovich [13] formula. We excluded the contact analysis to reduce running time and accelerate the stochastic analysis results. We are planning to apply the substructure technique which will allow us to include contact analysis to the simulation and improve stress results.

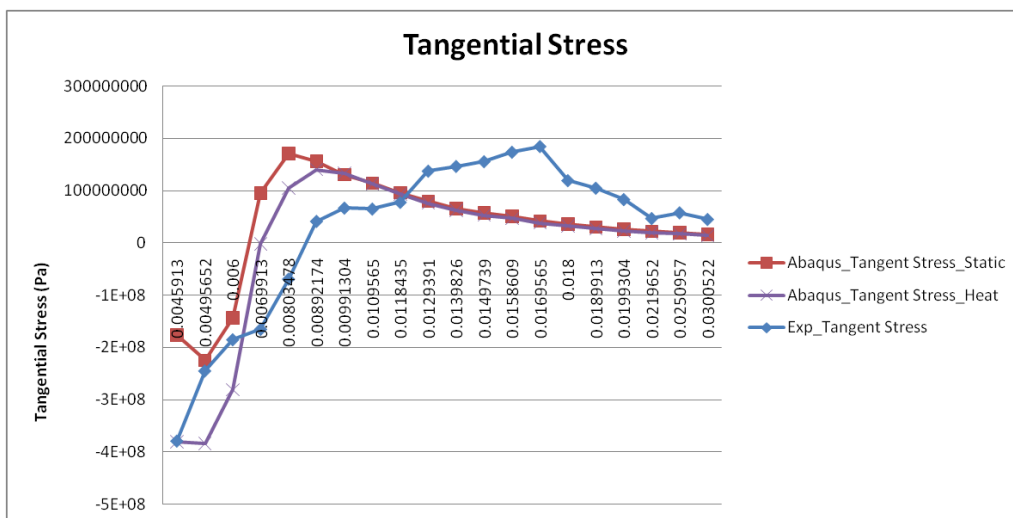


Figure 12. Residual Tangential Stress along the Distance from Rivet Centre.

The boundary conditions that were validated on the previous step, are applied on Coupon 1, which consists from panel (279mm x 50 mm x 15 mm) and stringer (279mm x 50mm x 8.5mm) and 6 rivets. Two models with different rivet-pitch are generated, one with minimum pitch (38 mm) (Figure 13.) and another with maximum pitch (48 mm) (Figure 14.). The stochastic process of the derived residual stress

due to riveting was studied by applying different temperature boundary conditions. The model is fixed at one end while the other end is fixed only in the z direction to simulate the real case scenario on the assembly line. Only half model is modelled making use of the symmetry in the boundary conditions.

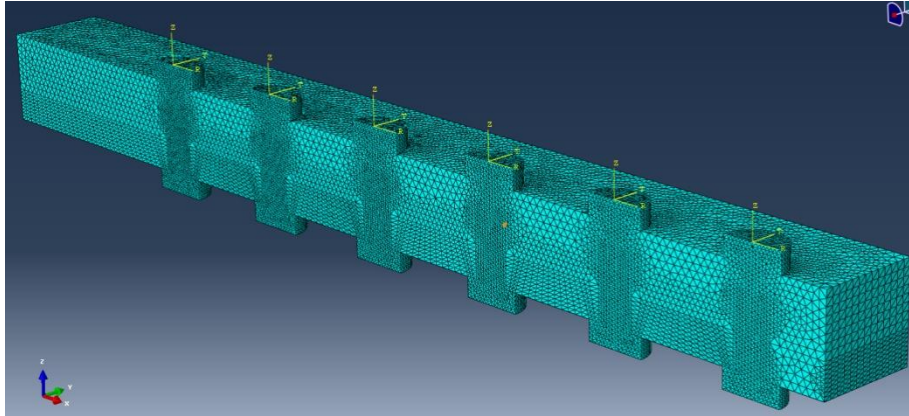


Figure 13. Coupon 1 with Min. Pitch.

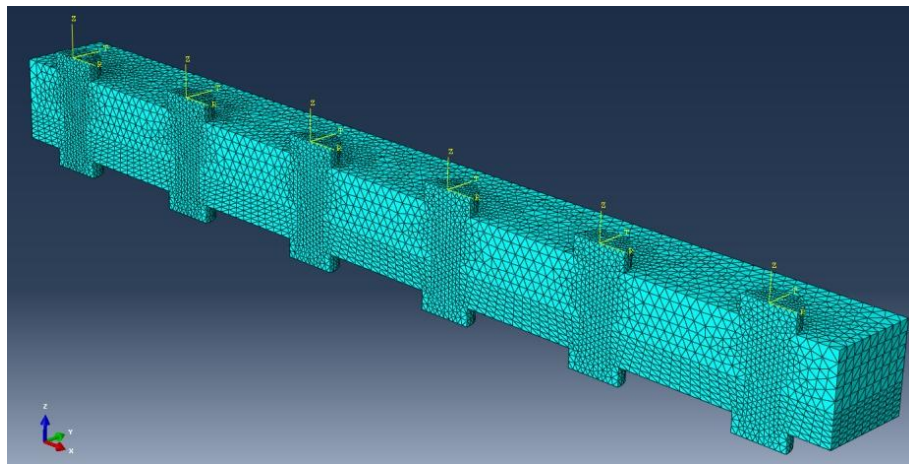


Figure 14. Coupon 1 with Max. Pitch.

5.2 Probabilistic Analysis

Different scenarios of probabilistic analyses were conducted in an effort to identify the influence of the applied temperature conditions on the panel growth. More specifically, the examined coupon was considered in two separate material configurations and two rivet pitch distances. The applied temperature conditions at each rivet for all the case studies were varied following a normal distribution with mean value 250 °C and standard deviation 10%. The total elongation of the coupon was measured at the edge and on the centreline.

Only two cases for different material selections for the stringer will be demonstrated, highlighting the variability on the results. More specifically, at the first scenario, the material type of the skin and the stringer was selected to be AA2024-T351 and AA2024-T3, respectively. Additionally, the minimum allowable pitch distance was considered. 500 Monte Carlo Simulations were performed, changing independently each of the temperature conditions and the derived histogram of the probability mass function and cumulative distribution function is depicted in Figure 15.

In the second case, the material type of the stringer was selected to be AA2050-T84 and considering the minimum allowable pitch distance, the derived histogram of the probability mass function and cumulative distribution function is depicted at Figure 16.

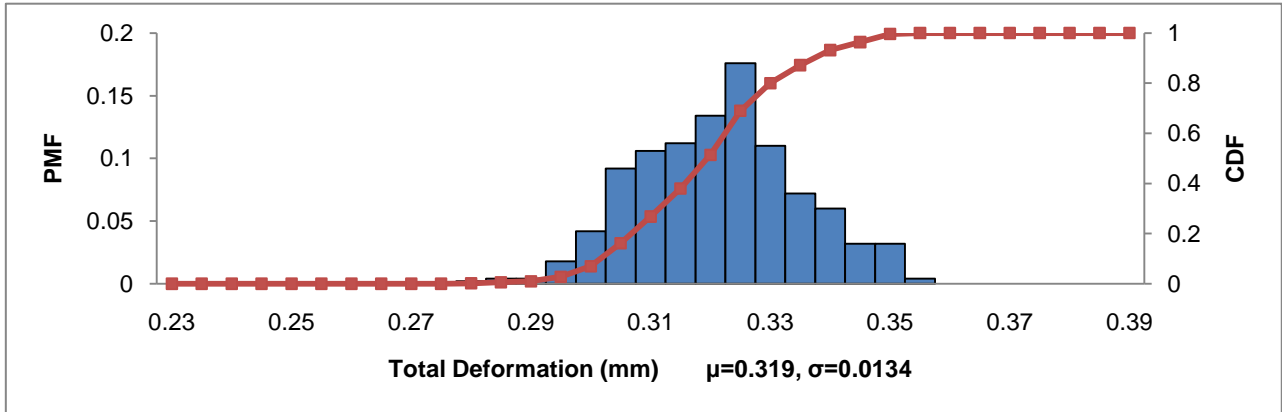


Figure 15: Probability Mass Function and Cumulative Distribution Function for material selection AA2024-T351/AA2024-T3 and minimum rivet pitch distances.

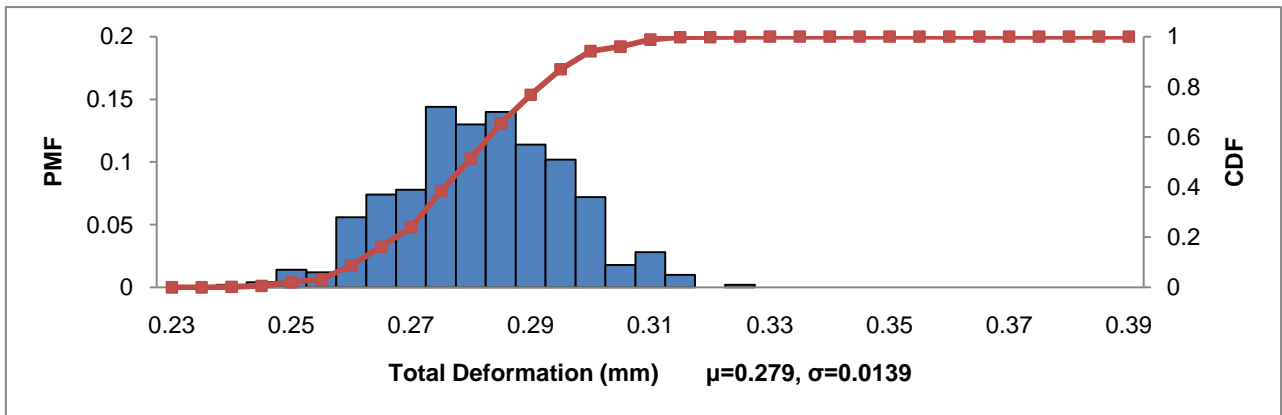


Figure 16: Probability Mass Function and Cumulative Distribution Function for material selection AA2024-T351/AA2050-T84 and minimum rivet pitch distances.

Through a comparison of Figures 15 and 16, it becomes apparent that the resulted distribution of the growth exhibited an asymmetrical form despite the normal distribution of the input parameters. Additionally, for the material configuration AA2024-T351/AA2050-T84 (material AA2050-T84 is stiffer than AA2024-T3) the mean value of the obtained growth was shifted towards to lower values, while the standard deviation of the elongation was almost the same for both cases and around 5%.

6.0 OPTIMISATION

6.1 Problem Definition

Multidisciplinary design optimization will be a key element in the future shaping of aerospace vehicles. Nowadays, the traditional single-discipline design gave rise to the robust multidisciplinary design [14]. This transition was assisted by modern advances in computational infrastructure and the developed sophistication of the numerical algorithms. Consequently, computation-intensive design problems are made feasible, involving complex analyses from various disciplines and a large parametric space. In aerospace applications, the multidisciplinary design optimization problem definition includes single or

multi-objective functions (from structures and/or aerodynamics disciplines) subject to constraints on performance characteristics.

This framework was applied on the VeLTA prototype, aiming to find the spanwise skin thickness of the wings that minimize the total mass of the aircraft subjected to flutter constraints. More specifically, considering that the cross section of the wing box has rectangular shape and splitting the wing into five segments, five design variables which corresponded to the thickness of the covers at the end of each segment were defined, namely tc_1 , tc_2 , tc_3 , tc_4 and tc_5 . These design parameters were subjected to upper and lower limits in an effort the spanwise skin thickness to uniformly reduce from the root to the tip of the wing. Additionally, a lower limit on the occurred flutter speed was set up as a constraint in order to avoid as possible dynamic instabilities. Finally, a single objective function was defined and related to the Maximum Take-Off Weight of the vehicle.

6.2 Design of Experiments

The design automation and verification of complex virtual prototypes is assisted using effective tools based upon computational experiments. Sampling techniques, such as Design of Experiments, help the engineer to debug the modelling process, ensure its integrity and identify the sensitivity of the model upon the design parameters [15]. Accordingly, in order to gain an insight on the variability of the objective function as well as of the flutter constraint, a full factorial sampling technique was set up and performed for the five design variables. The influence of the design parameters on the weight function and the flutter constraint is depicted at Figure 17 and 18, along with the corresponding surface plots with respect to the most critical variables. It is worth to mention that the weight of the wing box and as a result of the whole aircraft is depending upon all the parameters, while the flutter constraint is mainly affected from the skin thickness near the tip of the wing.

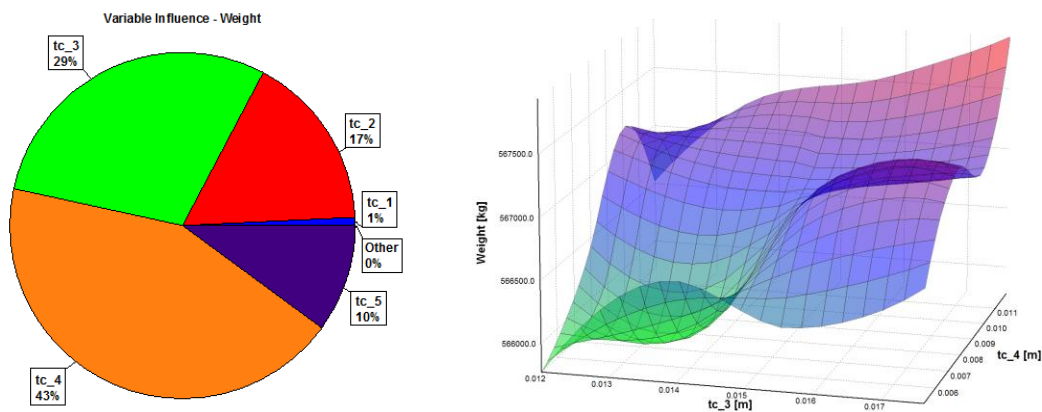


Figure 17: Influence of the design variables on the Weight function and surface plot of the Weight function with respect to variables tc_3 and tc_4 .

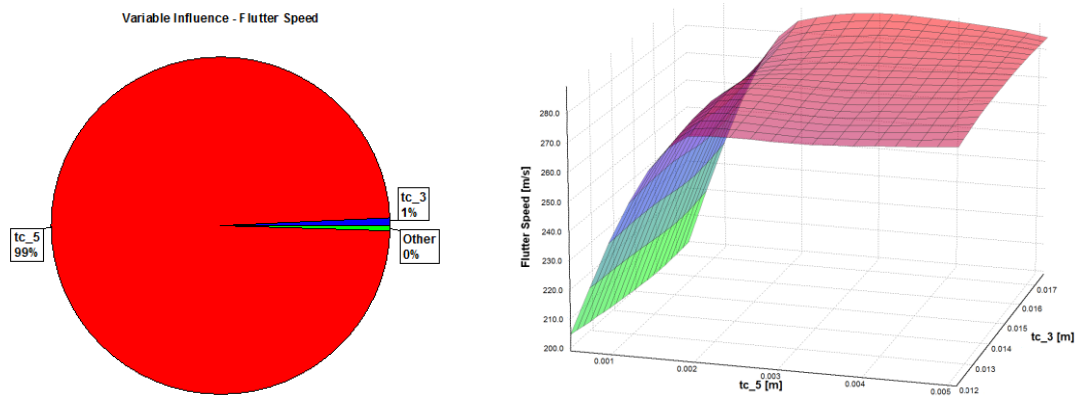


Figure 18: Influence of the design variables on the Flutter Speed constraint and surface plot of the Flutter Speed with respect to variables tc_3 and tc_5 .

6.3 Optimization Results

An important prospective of the Design of Experiments techniques lies upon the possibility in creating regression models that capture the actual behaviour of the virtual prototype. For multidisciplinary studies that are characterized by time-consuming simulations, the replacement of the actual model by a surrogate (Figure 19) appears as a necessity, aiming to reduce the design time and effort. For the examined optimization problem, a reliable and representative regression model was built exploiting the conducted computational experiments and using the Kriging method implemented within ModelCenter software [16]. Consequently, the calculation of the aircraft’s weight as well as of the flutter speed was replaced by “black-box” functions, reducing significantly the simulation time without affecting the accuracy of the results.

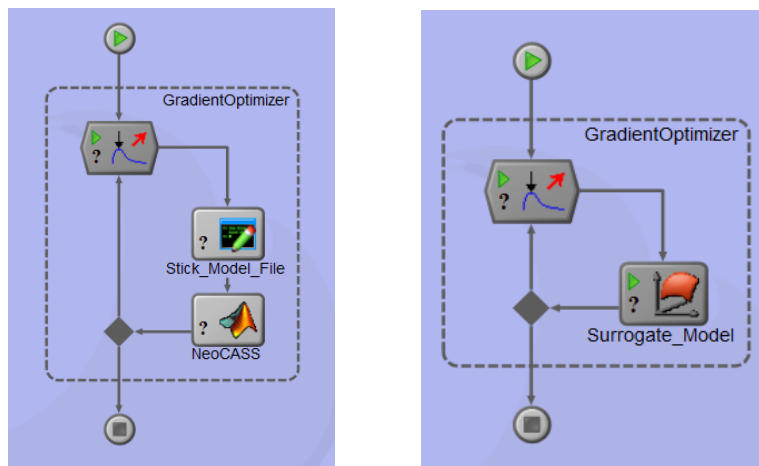


Figure 19: Actual and surrogate modelling.

Three different methods of the ModelCenter software were invoked for the solution of the examined optimization problem, including a Hill-Climbing algorithm (Gradient Method), an Evolutionary Algorithm (Darwin Method) and a hybrid approach (Design Explorer) which combines efficiently surrogate modelling and a gradient-based optimization method (SQP). All the built-in optimizers ended up to the same optimum values for the design parameters (Table 1) that led to weight reduction (up to 1 tonne), while maintaining the flutter speed above a certain limit (290m/s). It is worth to mention that in order to reduce the aircraft’s weight the first four variables reached their lower limits, while the fifth parameter reached the upper limit in an effort the vehicle to achieve higher flutter speed.

	tc ₁ [m]	tc ₂ [m]	tc ₃ [m]	tc ₄ [m]	tc ₅ [m]	Weight [kg]
Gradient Method	0.02119	0.01761	0.01491	0.00510	0.00265	565936.5
Darwin Method	0.02119	0.01761	0.01493	0.00510	0.00263	565936.9
Design Explorer	0.02119	0.01761	0.01489	0.00510	0.00265	565936.7

Table 1: Optimization results from different techniques.

7.0 MANUFACTURING

The assembly of aeroplane wings is a complex labour-intensive operation [17]. Planning and evaluation of an assembly of a wing is an important component of the design process. A well designed assembly process should take into account various factors such as optimum assembly time and sequence, tooling and fixture requirements, ergonomics, operator safety, and accessibility, among others [18]. It needs to meet many challenges on accuracy, efficiency, health and safety. Conventional methods of planning and development are no longer sufficient to speed up planning and evaluation processes, to reach ambitious budget targets and to manage the increasing complexity of new aircraft [19]. In development departments, the widespread use of CAD has led to a situation where today, the planning of assembly processes could be supplemented or completely substituted by virtual assembly technologies. The elimination of hardware or prototype phases not only cuts costs and time, but also makes it possible to take product decisions during early phases of development.

There are two main approaches to solve different aspects on the assembly planning in previous works by using virtual assembly techniques. The first approach is calculating the time and cost on different assembly sequences in a virtual environment. The second approach is using immersive Virtual Reality (VR) system to tackle ergonomics, health and safety, and accessibility in the assembly [20]. VR technology has evolved to a new level of sophistication during the last two decades. VR technology combines multiple human-computer interfaces to provide various sensations (visual, haptic, etc), which give the user a sense of presence in the virtual world. This makes VR a candidate tool for simulating tasks that require frequent and intuitive manual interaction such as assembly methods prototyping.

For the purposes of this work, a wing box and its trailing edge model of a Very Large Transport Aircraft (VeLTA) was developed to demonstrate the benefits of the virtual assembly in aerospace industry. The VeLTA is a generic concept design of a large transport aircraft which is being developed at the Virtual Engineering Centre (VEC). The wing assembly line is broken down into four key areas—skin panel assembly, structural wing assembly, wing equipping and paint. This paper describes the simulation of the installation of a flap track on the stage 3 wing assembly and focuses on the ergonomic aspect of the operation.

7.1 Materials and Methods

7.1.1 Hardware

In this study, an immersive VR system for the virtual assembly was constructed in VEC. The stereo display for the system was a dual projector blended ActiveWall as shown in Figure 20. The screen was 6 meters wide and 2 meters high. Two WUXGA active stereo projectors were placed at the back of the screen and provided a display of 3.6 million pixels (3390 horizontal and 1200 vertical). There was a 0.8m (450 pixels) blended area. The position of the operator in front of the stereo screen was tracked by 12 Vicon infrared tracking cameras. The stereo display is always related with the position of the operator. A nVisor SX111 HMD was used for personal stereo viewing and tracking the position and orientation of the

head. Head tracking for the HMD was implemented using magnetic trackers. A HAPTION haptic control device was used to generate force feedback during assembly tasks. While performing assembly tasks, the users could see their corresponding human model in virtual environment.

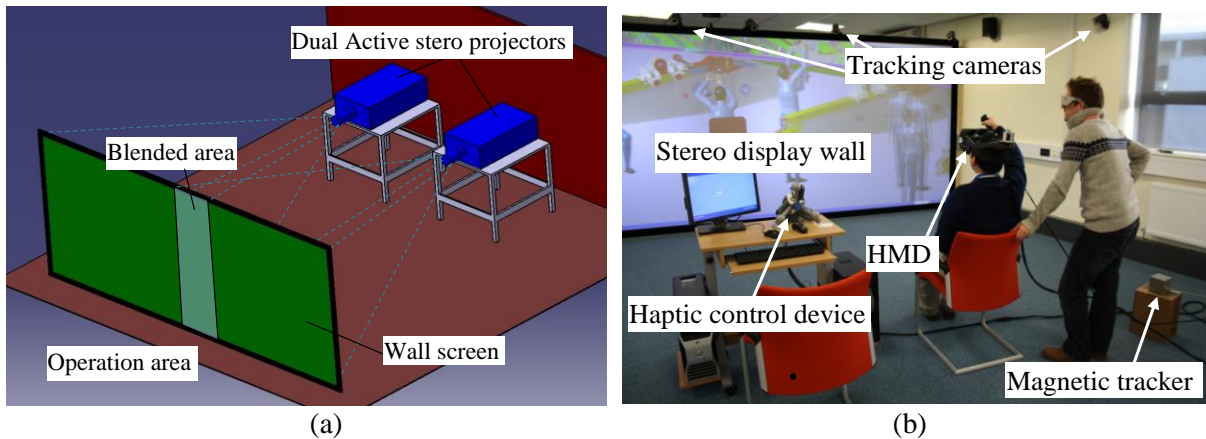


Figure 20. The immersive VR system for the virtual assembly.

7.1.2 Software

The software used here for investigating virtual assembly was Dassault Systemes DELMIA V5 R20 and HUMAN module. The use of V5 HUMAN ensures that products are designed from the perspective of the people who manufacture, maintain and operate them. The Rapid Upper Limb Assessment (RULA) analysis was used to calculate the ergonomic score for each manikin. The RULA analysis examines the following risk factors: number of movements, static muscle work, force, working posture, and time worked without a break. All these factors combine to provide a final score that ranges from 1 to 7.

- 1 and 2: (Green) Indicates that the posture is acceptable.
- 3 and 4: (Yellow) Indicates that further investigation is needed and changes may be required.
- 5 and 6: (Orange) Indicates that investigation and changes are required soon.
- 7: (Red) Indicates that investigation and changes are required immediately.

7.1.3 Assembly and simulation procedure

In stage 3 of the wing assembly, the wing box is placed down horizontally on the factory floor. Workers carry out the assembly tasks on a height of between one and two meters, as shown in Figure 21. In this study, No.6 flap track was chosen for the assembly simulation.

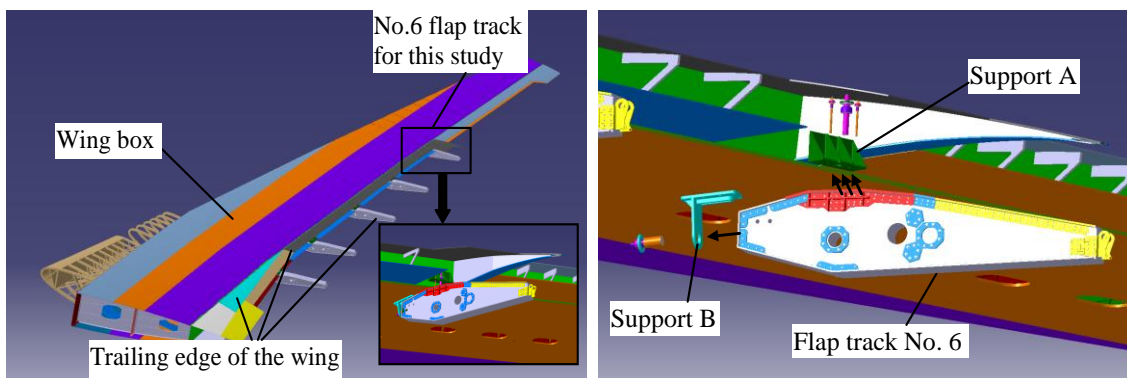


Figure 21. The structure of the wing box and the trailing edge, and the assembly task of the No.6 flap track.

7.2 Results

The assembly task is to install the flap track to Support A and Support B as shown in Figure 21. The total weight for the flap track is calculated as 230Kg in Delmia. Obviously, a lift device is needed to place the flap track to position as shown in Figure 22. Three workers carried out this assembly task and the position of each worker is also shown in Figure 22. The ergonomic scores of three workers were calculated and listed in Table 2. The colouring manikins were shown in Figure 22(a). The results show that the position of the Worker 1 is acceptable and the positions of the Worker 2 and 3 needed to be optimised.

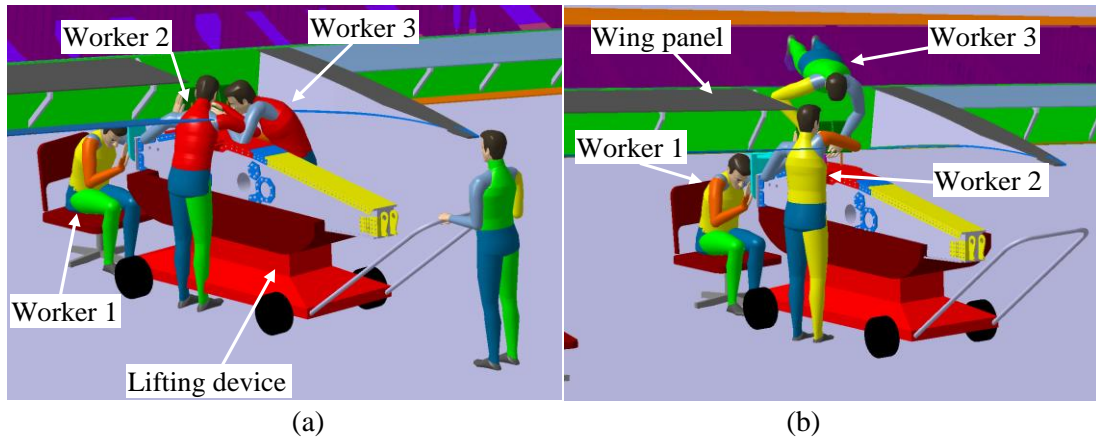


Figure 22. The coloured manikins for the assembly task (a) original (b) optimised.

To improve the ergonomics, the panels, which are on the top of the No.6 flap track, were removed. Worker 2 had more room to stand up straight to carry out the assembly task. Because of the narrow space, Worker 3 climbed up to the top of the wing and reached down to Support A as shown in Figure 22. The optimised scores are listed in Table 2. The ergonomic scores of Worker 2 and 3 reduced significantly.

Worker	Upper		Wrist				Leg	Final Score
	Arm	Forearm	Wrist	Twist	Neck	Trunk		
Task 2 worker 1	3	2	4	1	1	1	1	4
Task 2 worker 2	6	1	4	2	4	3	1	7
Task 2 worker 3	6	2	5	2	4	3	1	7
Optimised worker 2	2	1	4	1	2	1	1	4
Optimised worker 3	2	2	3	1	1	1	1	3

Table 2. The RULA scores for three workers before and after optimizing the assembly task.

7.3 Discussion and Conclusions

This study was carried out to provide an evaluation of the virtual assembly methods in aerospace industry using a generic large transport airplane wing model. The main purpose of the work was to use immersive VR system and Delmia software to tackle optimum assembly ergonomics, health and safety, accessibility, and fixture requirements in the wing assembly. In this assembly task, all the workers were working in ergonomic challenge positions. It did reflect the overall challenge facing the aerospace industry [17].

To reduce the ergonomic challenge, workers could change the access route to reaching the area for assembly tasks. As shown in Figure 22(b), the position of Worker 3 was changed from a standing position on the floor to a prostrate position on the top wing panel to carry out the operation. This also required changing the assembly sequence. The ergonomic scores were significantly reduced after these changes.

Virtual assembly techniques have widely applied in many industries [19,20]. The immersive VR system is more and more accepted as an effective tool to study ergonomics in virtual assembly because of its ability which allows people to interact with the virtual world [18]. The immersive VR system is particularly useful for the aerospace industry because the industry is labour intensive and has many health and safety issues. The installation of the flap track is a typical aerospace assembly task. This study has demonstrated that immersive virtual assembly system could foresee the ergonomic challenges in the assembly tasks and was able to reduce the risk effectively.

This study demonstrated that in aerospace industries, by using virtual assembly techniques, it is possible to take process design decisions during early phases of development. Virtual assembly techniques especially immersive VR systems are effective ways to tackle ergonomics, health and safety, accessibility, and fixture requirements in the assembly planning. Future work need to be carried out on quantifying the benefits of the VR.

8.0 CERTIFICATION OF CIVIL UAS: A VIRTUAL ENGINEERING APPROACH

8.1 Problem

The use of Unmanned Autonomous Systems (UAS) is becoming an increasingly routine activity in military theatres of operation, particularly for the oft-cited dull, dangerous and dirty missions. There is growing acceptance that UAS will find similar utility within the corresponding civilian missions and beyond. UAS technologies are maturing rapidly but the associated regulations to allow open access to civilian airspace are yet to be fully formulated. Current UK practice is therefore to allow UAS operation only in segregated airspace (airspace denied to all other potential users) or in non-segregated airspace but restricted to line-of-sight operations, below 400ft only. There is a growing need to develop a means by which UAS can operate alongside existing airspace users, in all classes of non-segregated UK airspace.

Regulatory guidance on how UAS might eventually achieve this aim in the UK is provided by Ref. [21] and projects such as ASTRAEA/ASTRAEA 2 [22] are working towards demonstrating the technologies that will be required to achieve both the guidelines and ultimately, the certification requirements. The likely solution for a route to certification of a UAS is that those elements of the aircraft that would form part of a piloted aircraft will be certified under the existing regulations (for example, [23]) whilst those elements of the aircraft designed to replace the pilot would be certified under, as-yet unpublished, UAS-specific regulations. The aim here, from a regulatory perspective, outlined in [21] would be to demonstrate that the safety of other airspace users is not compromised by the presence and/or proximity of a UAS.

The UAS community therefore finds itself with a paradox. Manufacturers require a set of certification standards against which they can design a UAS whilst regulators would ideally like to be able to appraise an already extant UAS. Virtual Engineering, which is the integration of product modelling with process modelling, provides a potential means to break this deadlock.

8.2 VEC Aims

The University of Liverpool's Virtual Engineering Centre (VEC) project aims to develop integrated Virtual Engineering (VE) processes, tools and techniques across the Product Life Cycle (PLC). The use of VE for modelling the integration of civil UAS into non-segregated UK airspace is the subject of a case study for the Test and Certification phases of the PLC. The research is being conducted in collaboration with BAE Systems – an industry partner of the VEC. By inserting a virtual prototype of a UAS into its virtual environment, the intention is to provide a capability that allows:

1. UAS developers and their suppliers to collaboratively capture design and certification requirements as early as possible in the PLC.
2. System suppliers access to development tools that would otherwise be unaffordable.
3. UAS developers to manage the risks associated with the certification process when integrating third-party software and hardware into a UAS.

8.3 Facilities

The architecture of the real-time networked simulation facilities (the core tool to be used for developing tools and techniques) that have been developed at the VEC, in conjunction with BAE Systems, is illustrated in Figure 23. This currently consists of a FLIGHTLAB [24] UAS (based upon the Grob airframe) and its associated subsystem(s) such as the decision making Agent and ground control station. The UAS can be immersed in virtual UK airspace via an air traffic control simulation. This generates realistic air traffic patterns that the UAS can then interact with. All of these individual components are connected via a central hub. The ultimate aim is that this hub will be able to link with external facilities such as the flight simulation facilities at the University of Liverpool (UoL) [25]. This would then allow, several real-time piloted simulation high-fidelity vehicle models to be injected into the virtual airspace local to the UAS to assess, for example, the performance of its decision making algorithms. The UAS simulation can then be displayed using X-plane as illustrated in Figure 24, or alongside the ATC simulation on the VEC 6.0 x 2.1 metre visualisation suite as illustrated in Figure 25.

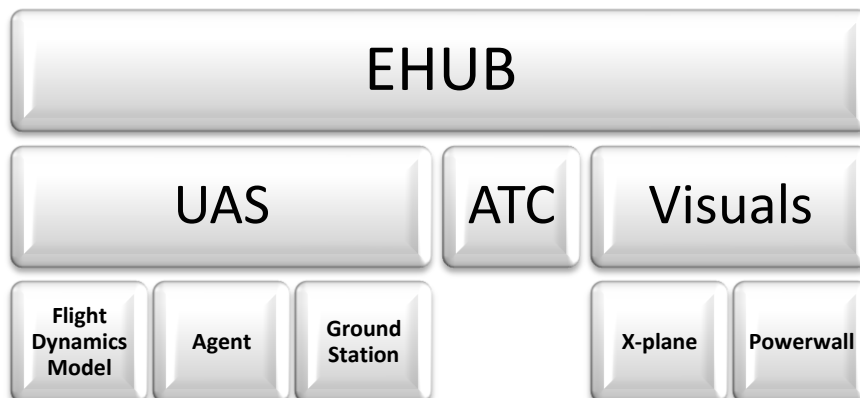


Figure 23. Structure of the VEC's Virtual Engineering Simulation Laboratory.

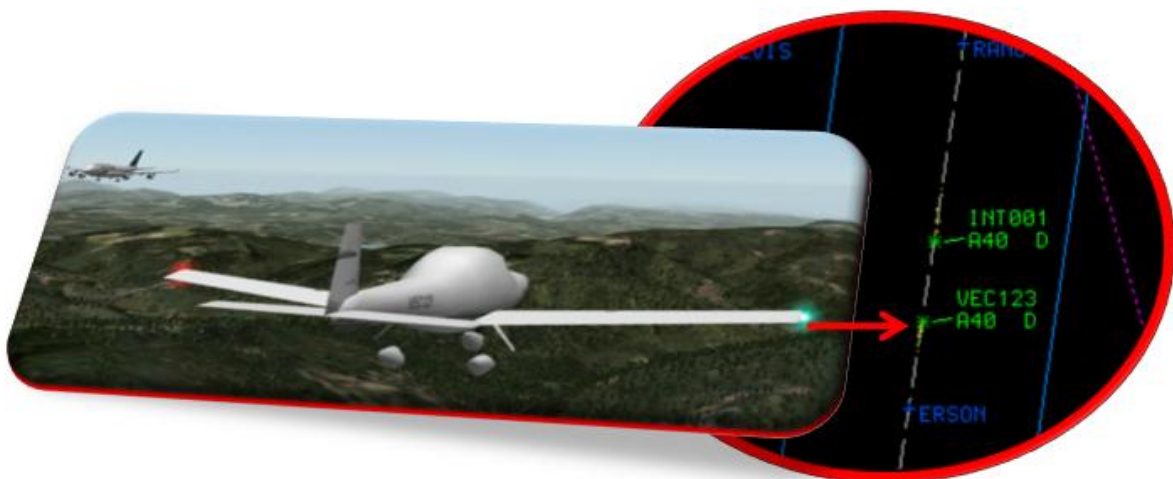


Figure 24. UAS VEC123 in Managed Airspace.



Figure 25. Visualisation of the Outside world as seen from a UAS camera and the Air Traffic Control Environment on the 6x2.1 metre Visualisation Screen at the VEC.

8.4 Proving Certification Requirements

The route to airframe and automatic flight control system certification is well established for manned aircraft. However, the regulations that must be adhered to have been developed over 100 years of manned flight. There is an implicit assumption within the regulations that a human will be on board the aircraft. For a UAS, this is not the case. Once the pilot is removed from the aircraft and made remote, Ref [21] indicates that, the UAS must:

- be equivalent to other airspace users: i.e. be able to operate within existing infrastructure such as ATC regulations
- be transparent to other airspace users: i.e. require no special considerations for operating in non-segregated airspace
- be no less safe than the equivalent manned aircraft.

The key difference between UAS and human-piloted aircraft is the autonomous Complex Flight Control System (CFCS), plus the systems directly associated with it (power supplies, etc.). Therefore, a vital part of providing evidence for certification is to show that this core autonomous control would make the same decisions as a human pilot/controller would make in a given situation [26], such that the autonomous CFCS must not increase the risk of mishap to other airspace users.

The VEC will be using the simulation facilities described in Section 8.3 to develop case studies which demonstrate how evidence of the CFCS meeting/not meeting certification requirements can be generated. Two example situations currently being assessed are:

- How the decision making processes within the CFCS can impact upon the frequency of an identified risk occurring. Agent-based programming and the associated formal methods [26] (in the form of an “intelligent” agent) are being used to examine this issue.
- How sensor models with various resolutions and capabilities will impact upon the UAS CFCS decision making process and hence the level of safety achieved.

9.0 VERIFICATION & VALIDATION

Virtual Engineering (VE) is concerned with integrated product and process modelling and the creation of virtual prototypes. Before making anything, the VE process aims to produce a verified design specification that meets the validated requirements. Confidence in the decisions derived from VE is directly related to the accuracy of the predictive capability of the product modelling on the one hand, and the robustness and

quality of the optimisation capability of the process modelling on the other. Accuracy, robustness and quality are critical in VE and are captured by the verification and validation (V&V) processes as outlined below:

- Verification involves checking that the outputs of the product and process models conform to the system design specification and is primarily a check on the correctness of the modelling relative to the design.
- The validation process checks if the design will work in practice and that the fully engineered product will meet the design requirements. In this sense, Validation is concerned with the accuracy of the predictive capability. Validation is also concerned with the quality and robustness of the optimisation process.

Both verification and validation are quantifiable processes that need criteria and associated test procedures to demonstrate compliance. However, unresolved issues persist within the modelling and simulation community pertaining to credibility of results and V&V processes e.g. risk, confidentiality and property rights, levels of uncertainty and fidelity, confidence and model maturity. Addressing these issues is a key contributor to the success of the VE approach.

The research described in this section has been undertaken as a joint activity between the Virtual Engineering Centre (VEC) and the University of Liverpool's (UoL's) ERSPC funded "*Lifting Standards: A Novel Approach to the Development of Fidelity Criteria for Rotorcraft Flight Simulators*" project [27]. Whilst Work Package 5 (WP5) of the VEC is examining issues related to Verification and Validation (V&V) generally for all virtual processes, the work of the *Lifting Standards* project is focussed on the direct application of V&V to rotorcraft simulation. In addition to the fidelity metric development described in this report, the analysis tools, methodologies and metrics developed in *Lifting Standards* will feed across into the VEC, where their applicability to the wider problem of V&V for virtual prototypes is being addressed.

9.1 Rotorcraft Simulation Fidelity

The expanding requirements for rotorcraft operations in harsh environments, e.g. emergency medical/law enforcement services and maritime/coast guard, along with the introduction of tilt-rotor aircraft into both civil and military service and the extensive replacement of large numbers of airframes dating from the 1960s and 1970s, are some of the challenges facing the rotorcraft industry today. These challenges are being met within the context of new environmental and safety constraints [28]. Successful completion of the conception-design-build-test / qualification-production-operation cycle of helicopters is highly dependent on the use of modelling and simulation, but fidelity is critical to confidence at early stages of the life cycle and requires the development and use of suitable Verification and Validation Metrics.

Flight simulators are extensively used in engineering design, development and flight training, and are an essential tool in the conceive-design-build and qualification processes of rotorcraft. However, simulators have an inherent flaw: despite their complexity and the use of state of the art components, they are not able to provide a fully coherent representation of reality and rely on providing a 'sufficiently realistic' illusion of flight to the pilot. How strong that "illusion" is may act as an indicator of the "fitness for purpose" of a simulator for a given use. In the context of training simulators, regulatory authorities have produced functional performance standards, along with associated training credits, to provide a framework for the acceptance of a synthetic training device. Documents such as JAR-STD 1H [29] and FAA AC120-63 [30] describe the qualifying criteria and procedure for rotorcraft flight training simulators and detail the component fidelity required to achieve a "fit for purpose" approval. Whilst these standards serve a vital role in the regulatory process, the influence of the cueing environment on pilot opinion during

qualification needs to be understood better. Currently there are no quantitative methods used to assess the fidelity of the overall system, with the pilot performing a task. The current development philosophy of the European JAR-STD 1H specification is that simulator requirements “*should be applied in practice and the lessons learned embodied in future amendments*”, providing an opportunity to incorporate new fidelity criteria when appropriate. It is the need to have objective measures of predicted fidelity, supplemented by subjective measures of perceived fidelity that is main focus of the *Lifting Standards* project. The approach follows the fundamental constructs of handling qualities engineering.

9.2 Lifting Standards: A Novel Approach to the Development of Fidelity Criteria for Rotorcraft Flight Simulators

The quantification of simulation fidelity underpins the confidence in the expanding use of flight simulation in design, in qualification support, and to provide safe and realistic environments for pilot training. The aim in quantifying the fidelity of the simulator then becomes one of understanding the effect that a change in the simulation environment will have upon the pilot’s ability to perform the task. A two stage approach for defining fidelity criteria for simulator qualification is being developed. Firstly, a quantitative basis for predicting fidelity using metrics, derived in part from handling qualities engineering. Secondly, perceptual fidelity metrics supplemented by a pilot fidelity rating scale, used to assign the perceived fidelity of the simulator.

This project involves collaboration with the Canadian Nation Research Council’s (NRC) Flight Research Laboratory and consists of two main phases. The first in February 2009 involved the collection of ‘benchmark’ test data from the NRC’s 412 Advanced Systems Research Aircraft (ASRA) (Figure 26) test aircraft and Liverpool’s HELIFLIGHT-R flight simulator (Figure 27). Features of HELIFLIGHT-R include:

- 12 ft visual dome with 3 x LCoS HD projectors on gimballed mounts to provide up to 210x70 deg. (field of view) FoV
- Interchangeable crew stations with front pilot and co-pilot seats and a rear engineer seat
- Moog FCS ECoL 8000 Q&C-Line electric control loading system four-axis control loading
- Moog MB/E/6dof/24/1800kg electric motion system
- Instructor-Operator Station PC
- Reconfigurable instrument panel displays (left and right primary flight displays, backup analogue displays and Head Up Display)
- the selective fidelity FLIGHTLAB [31] multi-body flight dynamics modelling environment

During the second phase of the programme in April 2011, handling qualities fidelity metrics derived in phase 1 were tested in comparative exercises with varying levels of fidelity. The metrics will be used to produce evidence-based validation for requirements within existing and emerging simulator standards.



Figure 26: NRC Bell 412 ASRA at Ottawa Airport.



Figure 27: HELIFLIGHT-R facility at Liverpool.

9.3 Methodology For Simulation Fidelity Based On Handling Qualities Engineering

In the field of Handling Qualities (HQ) engineering, two independent assessment processes are conducted, which combine to give the overall HQs of an aircraft. The practices adopted in the *Lifting Standards* project are drawn from the HQ specification, ADS-33E-PRF [32].

The first assessment process analyses the *predicted HQs* of the test aircraft. Predicted HQs are based around the analysis of clinical tests such as pulse, step, doublet and frequency sweep control inputs. HQ metrics have been developed to assess the full range of aircraft response, from low to high frequency and from small to large amplitude. Once the predicted HQ levels have been computed, the assessment can proceed to *assigned HQs*. In this stage, the test aircraft is flown in a range of manoeuvres that are representative of those that would be expected in the aircraft's operational role.

Much of the HQ methodology described above can be directly applied to the assessment of the fidelity of the flight simulator. Here, however, the goal is not to determine the level of HQs offered by the aircraft,

but rather to determine the difference between the simulator and flight test data for each of the metrics.

In the case of each of the predicted HQ metrics, the fidelity assessment is one purely focussed on the mathematical model of the test aircraft. For the assigned HQs, this is widened to consider not only the flight model, but also the cues that the pilot is able to detect while flying the task in the simulator. The primary generators of task cues within the simulator are the visual, motion, audio and inceptor force-feel systems.

As in the HQ assessment process, a comparison of the predicted and perceived fidelity [33, 34] results forms a key component of the overall fidelity assessment process. This stage is required in order to ensure not only that the predicted and perceived results are consistent, but that they are consistent for the same reasons in the simulator as they are in the flight test data.

A flow diagram representing the process for the assessment of predicted and perceived simulator fidelity is shown in Figure 28. As with the assessment of an aircraft's HQs, the process begins with a definition of the required purpose of the flight simulator, which will set the required level of fidelity. Once the purpose of the simulator has been defined, the predicted and perceived fidelity can be computed using a set of metrics such as those described in this paper.

The results from these tests feed into two decision points. The first question is; do the individual predicted and perceived fidelity metrics show a good match between flight and simulation? This is a key stage in the overall fidelity assessment process, as it highlights the overall quality of the simulation. The second question is related to the comparisons between predicted and perceived fidelity. In addition to verifying the overall fidelity of the simulator, the analysis at this point provides a further indicator as to the source of discrepancies between flight and simulation. If the predicted metrics show a good match, while the perceived metrics do not, then the indication is that the fidelity issues lie within the generation of the task cues and not the model.

If both questions can be answered positively then a decision can be made that the simulator is fit for its designed purpose and can be accepted for service. If, however, one of the fidelity requirements is not met, this would be an indicator that the simulator is not fit for purpose, and an upgrade, either to the cueing or the flight model or both, is required before the simulator can be accepted.

The perceived fidelity metrics relate to the task performance and pilot compensation. Task performance and workload metrics are useful for quantifying differences between flight and simulator. For task performance, these are; total task time, time spent within desired performance and percentage of the total manoeuvre time spent within the desired/adequate/beyond adequate performance tolerances. For the pilot's control compensation, the following metrics are used:

- a) Control attack which measures the size and rapidity of a pilot's control inputs, defined as:

$$attack = \frac{\dot{\eta}_{pk}}{\Delta\eta}$$

where η is the pilot's control deflection. The control attack is summarised using the following parameters:

- b) In the frequency domain, the following can be assessed:
- Root-Mean-Square (RMS) of the power spectral density in each control axis.
 - Cut-off frequency where 70% of the PSD has accumulated.

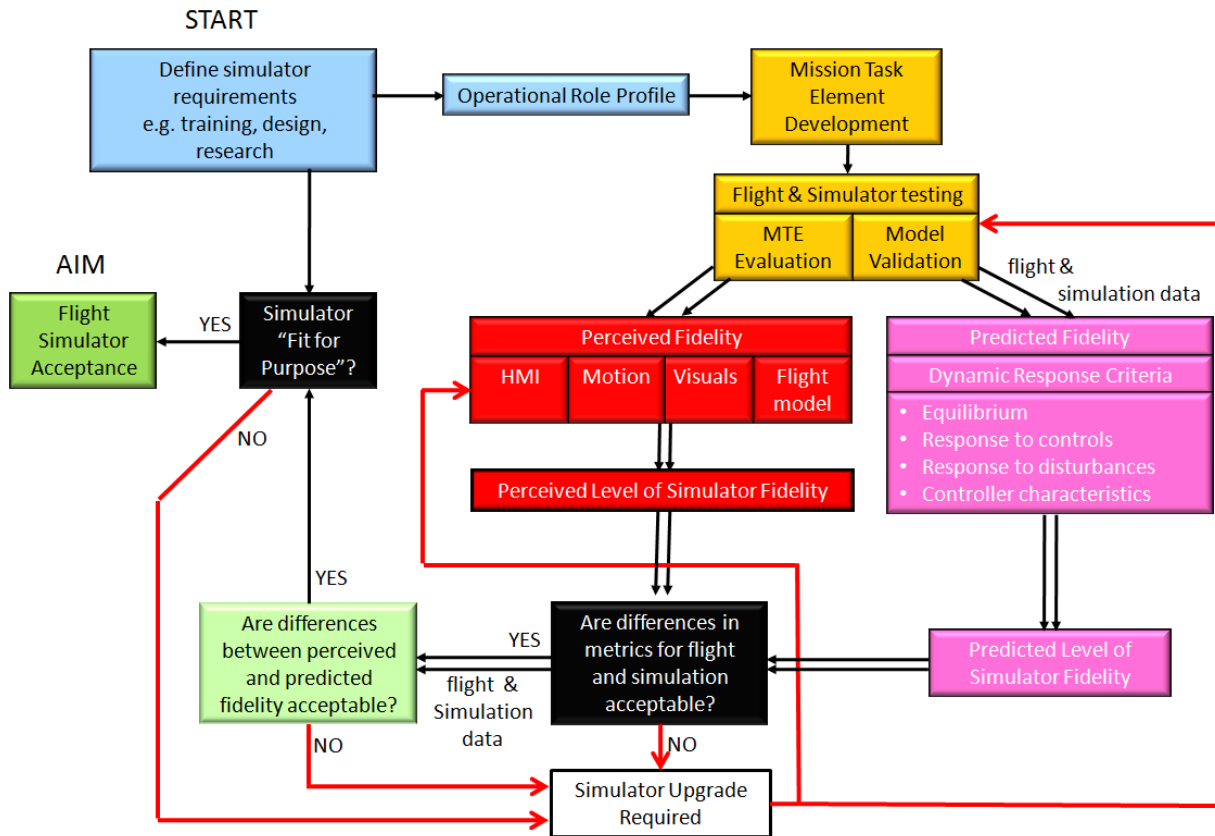


Figure 28: Methodology for Integrated Predicted and Perceived Simulator Fidelity Assessment.

The control attack and closed-loop quickness metrics have been shown to be sensitive to differences between flight and simulator. In particular, both the number of attack points and the mean attack rate exhibit a large difference between flight and simulation for almost all test points. It is hypothesised that un-modelled atmospheric disturbances and unsteady interactional aerodynamics contribute to the reduced activity in the simulator.

The *Lifting Standards* project has developed a number of parameters that are sensitive to differences between flight and simulation, and are therefore suitable for use as metrics of fidelity. For simulation to be truly representative of the real world, cueing and aircraft behaviour need to be sufficiently good that training is effective at skill development and retention. The flight simulation community has engaged with the concept of ‘fit for purpose’ for many decades and needs to continue to do so as technologies advance and the user aspirations of what can be achieved increase. Fidelity metrics, based on fundamental engineering science, need to advance ahead of the utilisation so that qualification standards development is properly supported. Work is required to fully establish cause and effect and to quantify the allowable discrepancies between flight and simulator; these are the subjects of ongoing research in the *Lifting Standards* project at Liverpool, together with the identification of a single, simple metric for fidelity assessment and the development of a perceived fidelity rating scale.

It is intended that the engineering metrics methodology developed within *Lifting Standards*, whilst directed at rotorcraft simulation fidelity, will be utilised in other VEC activities. Within the VEC, each work package case study will develop and exercise product and process modelling to produce the VPs, and it will be in these applications that virtual validation is applied. For example, the simulation model of the aircraft and its systems is the ‘product’ in a traditional V&V process and a key question here is “How

closely does the model match the ‘design’ (the real aircraft)?” Thus the techniques developed in *Lifting Standards* on predicted fidelity requirements will read across directly to the VEC work on product model validation.

10.0 CONCLUSIONS

A range of very different examples of the use of Virtual Engineering involving the development of Virtual Prototypes, often through the use of Multidisciplinary Design Optimisation, undertaken at the Virtual Engineering Centre have been demonstrated. It has been shown that the use of Virtual Engineering can be used to optimize designs of complex systems and to reduce significantly the amount of experimental testing that is required.

11.0 ACKNOWLEDGMENT

This work is supported through the Virtual Engineering Centre (VEC), which is a University of Liverpool initiative in partnership with the Northwest Aerospace Alliance, the Science and Technology Facilities Council (Daresbury Laboratory), BAE Systems, Morson Projects and Airbus (UK). The VEC is funded by the Northwest Regional Development Agency (NWDA) and European Regional Development Fund (ERDF) to provide a focal point for virtual engineering research, education and skills development, best practice demonstration, and knowledge transfer to the aerospace sector.

12.0 REFERENCES

- [1] UK Aerospace International Strategy 2010, UK Trade & Investment, May 2010.
- [2] <http://www.incose.org/practice/fellowconsensus.aspx> Accessed April 2011
- [3] Hubka, V., “*Principles of Engineering Design*”. Zürich: Heurista 1987. First Edition Butterworth 1982.
- [4] www.incose.org.uk, INCOSE handbook V3, 2006 Accessed April 2011
- [5] A. Johnston and P. Hubert (1994), Effect of Processing Variables on Springback of Composite Angles. *A Report to the Boeing Company*.
- [6] T.A. Bogetti and J.W. Gillespie Jr. (1992), “Process-Induced Stress and Deformation in Thick-Section Thermoset Composite Laminates”, *Journal of Composite Materials* 26 (5), 626-660.
- [7] Johnston, A. A. (1997), An Integrated Model of the Development of Process-Induced Deformation in Autoclave Processing of Composite Structures. PhD dissertation, University of British Columbia.
- [8] D. Scida, Z. Aboura, M.L. Benzeggagh, and E. Bocherens (1997), "Prediction of Elastic Behaviour of Hybrid and Non-Hybrid Woven Composite", *Journal of Composite Science and Technology* 57, 1727-1740.
- [9] Cavagna, L., Da Ronch, A. and Ricci, S., “*NeoCASS Next generation Conceptual Aero Structural Sizing*,” Dipartimento di Ingegneria Aerospaziale, Politecnico di Milano, 2009.
- [10] Nash, S. M., and Rogers, S. E., “*Numerical Study of a Trapezoidal Wing High-Lift Configuration*,” SAE-1999-01-5559, October 1999.
- [11] M.E. Fox, and P.J. Withers (2007), "Residual Stresses in and around Electromagnetically Installed Rivets Measured using Synchrotron and neutron diffraction", *Journal of Neutron Research* 15 (3), 215-223.
- [12] Kaniowski, J., Jachimowicz, J. Methods for FEM Analysis of Riveted Joints of Thin-Walled Aircraft Structures Within The Imperja Project. 25th ICAF symposium, Rotterdam May 2009.
- [13] Yuncu, H. Thermal Contact Conductance of Nominally Flat Surfaces. *Journal of Heat Mass Transfer* Vol. 43, pp 1-5, 2006.
- [14] Padmanabhan, D., “*Reliability-Based Optimization for Multidisciplinary System Design: New Approaches and Applications*,” Saarbrücken, Germany: VDM Verlag Dr. Müller, 2011.
- [15] Forrester, A., Sóbester, A. and Keane, A., “*Engineering Design via Surrogate Modelling: A Practical Guide*,” Chichester, United Kingdom: John Wiley & Sons Ltd, 2008.
- [16] ModelCenter v9.0, *DesignProcessOptimization Software*, Phoenix Integration Inc., Blacksburg, Virginia, 2010.
- [17] Rooks, B., *Automatic wing box assembly developments*. *Industrial Robot: An International Journal*, 2001. 28(4): p. 5.

- [18] Seth, A., Vance, Judy.M., Oliver, James.H., *Virtual reality for assembly methods prototyping: a review*. Virtual Reality SI: Manufacturing and construction, 2010. DOI: 10.1007/s10055-009-0153-y.
- [19] Wohlke, G., Schiller, Emmerich., *Digital planning validation in automotive industry*. Computers in industry, 2005. **56**: p. 12.
- [20] Ding, Z.Y, Hon, K.K.B., Shao, F., *A virtual assembly approach for product assemblability analysis and workplace design*. 21st CIRP Design Conference 2011.
- [21] *CAP722 - Unmanned Aircraft System Operations in UK Airspace - Guidance*. 6th April 2010, Directorate of Airspace Policy, Civil Aviation Authority: London.
- [22] Astraea: <http://www.uavs.org/astraea>
- [23] *Certification Specifications for Large Aeroplanes CS-25, Amendment 8*. 2009: European Aviation Safety Agency.
- [24] Padfield, G.D., White, M.D., *Flight Simulation in Academia; HELIFLIGHT in its first year of operation*, The Aeronautical Journal of the Royal Aeronautical Society, Sept, 2003.
- [25] Duval, R.W., *A Real-Time Multi-Body Dynamics Architecture for Rotorcraft Simulation*, The Challenge of Realistic Rotorcraft Simulation, RAeS Conference, London, November 2001.
- [26] Clarke, E., M., Wing, J., M., et al., *Formal Methods: State of The Art and Future Directions*, ACM Computing Surveys, Vol. 28, No. 4, December 1996.
- [27] White, M. D., Perfect, P., Padfield, G.D., Gubbels, A. W. and Berryman, A. C., "Acceptance testing of a rotorcraft flight simulator for research and teaching: the importance of unified metrics." Proceedings of the 35th European Rotorcraft Forum, Hamburg, Germany, September 2009.
- [28] anon., "Strategic Research Agenda, Volume 1", Advisory Council for Aeronautics Research in Europe, October 2002.
- [29] anon., "JAR-STD 1H, Helicopter Flight Simulators", Joint Aviation Authorities, April 2001.
- [30] anon., "FAA Advisory Circular AC120-63, Helicopter Simulator Qualification", Federal Aviation Authority, November 1994.
- [31] DuVal, R.W., "A Real-Time Multi-Body Dynamics Architecture for Rotorcraft Simulation", The Challenge of Realistic Rotorcraft Simulation, RAeS Conference, London, November 2001.
- [32] anon., "ADS-33E-PRF, Handling Qualities Requirements for Military Rotorcraft", US Army, March 2000.
- [33] White, M. D., Perfect, P., Padfield, G.D., Gubbels, A. W. and Berryman, A. C., "Progress in the Development of Unified Fidelity Metrics for Rotorcraft Flight Simulators" Proceedings of the 66th Annual Forum of the American Helicopter Society, Phoenix, AZ, May 2010.
- [34] Perfect, P., White, M. D., Padfield, G.D., Gubbels, A. W. and Berryman, A. C., "Integrating Predicted and Perceived Fidelity for Flight Simulators" Proceedings of the 36th European Rotorcraft Forum, Paris, France, September 2010.